8868

NASA
Technical
Paper
2578

June 1986

Oxidation and Emittance of Superalloys in Heat Shield Applications

Karl E. Wiedemann,
Ronald K. Clark,
and Jalaiah Unnam

NASA

NASA Technical Paper 2578

1986

Oxidation and Emittance of Superalloys in Heat Shield Applications

Karl E. Wiedemann
Analytical Services and Materials, Inc.
Hampton, Virginia

Ronald K. Clark
Langley Research Center
Hampton, Virginia

Jalaiah Unnam
Analytical Services and Materials, Inc.
Hampton, Virginia

National Aeronautics
and Space Administration

Scientific and Technical Information Branch

Use of trade names or names of manufacturers in this report does not constitute an official endorsement of such products or manufacturers, either expressed or implied, by the National Aeronautics and Space Administration.

Symbols and Abbreviations

$M_{b,\lambda}(\lambda, T)$	spectral emissive power of a blackbody at temperature T and wavelength λ
α, γ, γ'	phase identification
$\epsilon(t, T)$	total normal emittence at temperature T
$\epsilon(\lambda)$	room-temperature spectral near-normal emittance at wavelength λ
θ	Bragg angle
λ_1, λ_2	lower and upper wavelength limits, respectively, of experimental data
$\Delta\lambda$	wavelength increment of experimental data
EDXA	energy-dispersive X-ray analysis
HYMETS	hypersonic materials environmental test system
ODS	oxide dispersion strengthened
R.I.	relative intensity
SEM	scanning electron microscopy
TEM	transmission electron microscopy
TPS	thermal protection system
XRD	X-ray diffraction

Summary

Recently developed superalloys that form alumina coatings have a high potential for heat shield applications for advanced aerospace vehicles at temperatures above 1095°C. Both INCOLOY[1] alloy MA 956, an iron-base oxide-dispersion-strengthened alloy, and CABOT[2] alloy No. 214, an alumina-forming nickel-chromium alloy, have good oxidation resistance and good elevated temperature strength. The oxidation resistance of both alloys has been attributed to the formation of a thin alumina layer (α-Al_2O_3) at the surface. Emittance and oxidation data were obtained for simulated Space Shuttle reentry conditions using a hypersonic arc-heated wind tunnel. The surface oxides and substrate alloys were characterized using X-ray diffraction and scanning and transmission electron microscopy with an energy-dispersive X-ray analysis unit. The mass loss and emittance characteristics of the two alloys are discussed.

Introduction

Radiatively cooled metallic heat shields are candidates for the thermal protection system (TPS) of advanced reusable reentry vehicles. Among the important material requirements for this application are long-term oxidation resistance, surface emittances of 0.8 or higher, low catalytic activity of the surface to the recombination of dissociated oxygen and nitrogen present in the boundary layer, and high-temperature strength (refs. 1 and 2). Preliminary results have indicated that except for the low catalytic activity, commercially available alloys of the nickel-chromium family might meet these performance requirements for temperatures up to about 1095°C (refs. 3 to 5). For temperatures above 1095°C, however, the strength and oxidation resistance requirements have led to consideration of more advanced materials such as oxide-dispersion-strengthened (ODS) alloys and superalloys that form protective surface coatings in oxidizing environments. INCOLOY alloy MA 956 (MA 956) and CABOT alloy No. 214 (Cabot-214) were selected as alloys representative of advanced materials that might be suitable for TPS applications at temperatures above 1095°C.

MA 956 is an ODS, Fe-Cr-Al-Ti alloy produced by mechanical alloying (ref. 6). This alloy is strengthened by a yttrium oxide dispersoid that remains stable at temperatures up to the melting point of the material. This alloy combines strength at high temperatures with excellent resistance to oxidation, carburization, and hot corrosion. Good dynamic oxidation resistance of MA 956 to reentry conditions was demonstrated by reference 7. The favorable corrosion resistance results from the formation of a highly adherent alumina film. The catalytic activity of MA 956 exposed to reentry conditions was also shown to be lower than that of a nickel-chromium alloy (ref. 7).

Cabot-214 is a wrought, Ni-Cr-Al-Fe alloy that has excellent oxidation resistance at high temperatures. Its superior oxidation resistance is attributed to the tenacious and protective alumina film that forms at the surface.

The present research investigated the oxidation characteristics and radiative properties of MA 956 and Cabot-214 for simulated Space Shuttle reentry conditions. Oxidation and emittance data were obtained for specimens exposed to simulated reentry conditions at a surface temperature of 1095°C using a hypersonic arc-heated wind tunnel. The surface oxides and substrate alloys were characterized using X-ray diffraction (XRD), scanning electron microscopy (SEM) with an energy-dispersive X-ray analysis (EDXA) unit, and transmission electron microscopy (TEM) with an EDXA unit. Mass change measurements and emittance measurements were made on the specimens exposed to simulated reentry conditions.

Experimental Procedures

Test Specimens and Exposure Facility

Test specimens of MA 956 and Cabot-214 were stamped from 0.6-mm-thick sheet and 0.3-mm-thick sheet, respectively. The specimens were disks 25 mm in diameter with three 5- by 5-mm radial projections spaced every 120° around the disk for mounting the specimens during simulated reentry testing. Table I gives the nominal chemical analyses of the materials as provided by the vendor.

The specimens of both alloys were heat-treated to form a submicron alumina layer at the surface that would provide oxidation protection for the material. The specimens were prepared for heat treatment by cleaning them thoroughly to assure that they were free of oils and then by glass-bead blasting. (The bead blasting produces a highly energized surface which, when oxidized, forms a uniform alumina layer.) Subsequently, the Cabot-214 specimens were heated in a reduced-oxygen atmosphere (H_2 with −70°C dew point) at 1095°C for 2 hr, and the MA 956 specimens were heated in an oxidizing atmosphere (air) at 1095°C for 2 hr. The very low oxygen atmosphere for the Cabot-214 specimens functioned as a reducing environment for α-Cr_2O_3 and as an oxidizing environment for α-Al_2O_3 so that α-Al_2O_3 was the preferred oxide formed at the surface.

[1] INCOLOY: Trademark of Inco Alloys International, Inc.

[2] CABOT: Trademark of the Cabot Corporation.

Specimens were exposed to 0.5-hr cyclic oxidation tests at 1095°C in the hypersonic materials environmental test system (HYMETS) at the Langley Research Center, which provides a high-temperature flowing-air environment simulating "Space Shuttle type" reentry conditions. The HYMETS facility is a 100-kW constrictor arc-heated wind tunnel. Figure 1 shows a schematic diagram of the test setup, which consists of a segmented constrictor arc heater, a test chamber with three model insertion stings, and continuous-duty vacuum pumps. Specimens were mounted on stagnation model adaptors attached to the insertion stings. Another sting contained a water-cooled heating rate and pressure probe that was used to measure the cold-wall heating rate and the surface pressure. The test gas was a mixture of air plus nitrogen and oxygen in ratios equivalent to air. High-purity nitrogen was introduced at the downstream end of the cathode, and air and high-purity oxygen were introduced in the plenum and mixing chamber.

The HYMETS nominal operating conditions for simulated reentry testing of the specimens are given in table II. The test conditions utilized here did not provide for full simulation of the Space Shuttle reentry environment. The heat flux, the most critical response parameter, was representative of the reentry environment, but the surface pressure and free-stream enthalpy were one-half to one-fourth the levels actually encountered on Space Shuttle reentry.

Analysis of Oxidation

Weight changes of specimens were determined by weighing specimens before and after simulated reentry exposure. These weight changes were normalized to the total surface area of the specimen. The morphology of specimen oxides was studied using scanning electron microscopy, energy dispersive X-ray analysis, X-ray diffraction analysis, and transmission electron microscopy.

Radiative Property Measurement

Room-temperature, near-normal reflectance measurements were made on preexposure and postexposure specimens using a Gier Dunkle DB100 reflectometer, a Perkin-Elmer Model 330 spectrophotometer with a Hitachi Model 320 integrating sphere (60-mm diameter), and a Gier Dunkle Model HCDR 3 heated-cavity reflectometer. The DB100 reflectometer measured the total room-temperature reflectance. The spectrophotometer with an integrating sphere was used to make spectral reflectance measurements over the wavelength range from 0.875 to 2 μm, and the heated-cavity reflectometer was used to make spectral reflectance measurements over the wavelength range from 2 to 25 μm. The reflectance data were used with Kirchhoff's law to arrive at corresponding values of emittance. The spectral data were then integrated numerically using the following equation:

$$\epsilon(t,T) = \frac{\sum_{\lambda_1}^{\lambda_2} \epsilon(\lambda)\ M_{b,\lambda}(\lambda,T)\ \Delta\lambda}{\sum_{\lambda_1}^{\lambda_2} M_{b,\lambda}(\lambda,T)\ \Delta\lambda} \qquad (1)$$

where $\epsilon(t,T)$ is the total normal emittance at temperature T, λ_1 and λ_2 are, respectively, the lower and upper wavelength limits of the experimental data, $\epsilon(\lambda)$ is the room-temperature spectral near-normal emittance at wavelength λ, $M_{b,\lambda}(\lambda,T)$ is the spectral emissive power of a blackbody at temperature T and wavelength λ, and $\Delta\lambda$ is the wavelength increment of the experimental data.

Results and Discussion

Oxidation Characteristics

Weight changes after reentry exposure were measured for both alloys. The weights gained were comparable. (See fig. 2.) For long exposure times the progressive weight changes became very small, a result indicating that a protective oxide layer had been developed on both alloys.

These weight changes were small when contrasted with alloys that failed to develop a protective oxide layer such as INCONEL[3] alloy 617 (Inconel 617). (See comparative data in fig. 3.) Under identical test conditions Inconel 617 lost weight because of the loss of chromium (ref. 8), whereas MA 956 and Cabot-214 gained weight because of the formation of a stable oxide.

X-ray diffraction analysis of the oxidized alloys (see table III) shows that the principal oxidation product was corundum (α-Al_2O_3). MA 956 also showed a complex hematitelike oxide, α-$(Fe,Al,Cr,Ti)_2O_3$, after the first reentry cycle. After 7.5 hr of reentry exposure, Cabot-214 showed contamination of the corundum by chromium oxide.

In MA 956, hematite and corundum were present before any reentry exposure. (See fig. 4.) These had been formed during the oxidizing heat treatment. The hematite peak was shifted to higher angles, an effect indicating a solid solution of this phase with oxides of titanium and aluminum. The corundum peak was near the peak position for pure corundum but showed a slight shift to lower angles, an outcome indicating a solid solution of this phase with

[3] INCONEL: Trademark of Inco Alloys International, Inc.

small amounts of the oxides of iron, chromium, or titanium. After the first 0.5-hr reentry cycle, the hematite peak was smaller and the corundum peak was slightly larger. After 7.5 hr of reentry exposure, the hematite had disappeared and the corundum peak, which had continued to become larger, showed a perceptible shift to lower angles that corresponded to 2 percent chromium oxide and 2.5 percent iron oxide, as determined by EDXA of individual crystals in the TEM.

The X-ray diffraction patterns for Cabot-214 are shown in figure 5. Corundum was present in all three patterns. In the pattern for 0-hr reentry exposure, there was a slight increase in the X-ray intensity over a broad region midway between the 2θ positions (where θ denotes the Bragg angle) for α-Cr_2O_3 and α-Al_2O_3. This was a statistically significant signal that was attributed to a small quantity of chromium-aluminum oxide solid solution having a range of composition centered at 50 molar percent α-Al_2O_3 and 50 molar percent α-Cr_2O_3. After the first 0.5-hr reentry cycle, the chromium-aluminum oxide solid solution had disappeared and the corundum peak had begun to show compositional broadening toward lower angles, a result indicating the formation of a solid solution with chromium oxide. After 7.5 hr of reentry exposure, considerable contamination of the corundum by chromium was evident. Analysis of this compositional broadening using the technique described in reference 9 indicated that 50 molar percent α-Cr_2O_3 was present in the corundum solid solution at the metal-oxide interface and none was present at the surface. This chromium oxide gradient was probably due to the formation of volatile CrO_3 at the surface (ref. 10). The small shift in the corundum peak of MA 956 and the extensive compositional broadening of the corundum peak of Cabot-214 can be rationalized on the basis of the limited solubility of hematite in corundum and the complete solubility of eskolaite (α-Cr_2O_3) with corundum (ref. 11).

Before any reentry exposure, the oxide layer on MA 956 appeared to be a nearly continuous array of small corundum and hematite spheres in the SEM. (See fig. 6.) After the first 0.5-hr reentry cycle, small and large spheres were seen. The EDXA (see table IV(a)) indicated that the small spheres were rich in aluminum and the large spheres were rich in iron. This specimen had a reddish tinge that may have been due to the hematite. After 7.5 hr of reentry exposure, the large spheres had disappeared. Thin flakes projecting from the corundum layer were visible. Extraction replicas taken from this specimen and observed in the TEM suggested that the flakes were α-Al_2O_3. Needlelike particles were also observed in the extraction replicas. The EDXA of these needles indicated that they consisted of 92 to 98 percent titanium oxide and 2 to 8 percent iron oxide. X-ray and electron diffraction analyses indicated that the needles had the anosovite ($TiO_2 \cdot Ti_2O_3$) structure.

Before any reentry exposure, the oxide layer on Cabot-214 appeared to be partially covered by "sheetlike" platelets of oxide that were 2 to 5 μm in width. (See fig. 7.) The EDXA (see table IV(b)) indicated that there were compositional differences between the light and dark regions. After the first 0.5-hr reentry cycle, there still appeared to be thin spots in the oxide layer. After 7.5 hr of reentry exposure, however, the oxide layer appeared to be uniform.

Radiative Properties

Table V presents data for individual specimens including simulated reentry exposure time and total near-normal emittance results determined from room-temperature reflectance data. Room-temperature and 1095°C emittance data before and after exposure to simulated reentry conditions are tabulated. Two sets of room-temperature emittance data are shown. The data sets labeled "DB100" were calculated from room-temperature total reflectance measurements made with a Gier Dunkle DB100 reflectometer. (The sum of emittance and reflectance is unity for an opaque specimen.) The data sets labeled "summed" (at room temperature and 1095°C) were calculated from the room-temperature spectral reflectance data using equation (1). The room-temperature emittance derived from the spectral data was about 0.03 greater than the values determined with the DB100. The greater value of total emittance from the spectral data resulted from the fact that the spectral apparatus covered a wider wavelength range (from 0.875 to 25 μm) that included regions of higher emittance than does the DB100 (from 10 to 15 μm).

Figures 8 and 9 show the change in spectral emittance of MA 956 and Cabot-214, respectively, with exposure to simulated reentry conditions. Both alloys experienced changes in spectral emittance with reentry testing at wavelengths greater than 10 μm that were attributed to changes in the oxide compositions and structure. In the wavelength region of greatest significance for radiative heat transfer in heat shield applications (less than 10 μm), the emittance of both alloys varied with wavelength in a fashion more orderly than at longer wavelengths. The data in table V show that the total near-normal emittance of MA 956 was about 0.70 and did not change appreciably with exposure to simulated reentry conditions, and the total near-normal emittance

of Cabot-214 decreased slightly with exposure to simulated reentry conditions from about 0.65 to about 0.57.

The spectral characteristics of both MA 956 and Cabot-214 were the result of multiple phenomena. The very thin oxide layer at the surface was primarily α-Al_2O_3 which has a uniformly high transmittance at wavelengths below 10 μm (ref. 12), with the result that the radiative properties in that wavelength range were governed primarily by the substrate. At longer wavelengths the transmittance of the oxide layer was low (ref. 12), with the result that the radiative properties were determined by the properties of the oxide and the substrate.

Figure 10 shows a comparison of the high-temperature total near-normal emittance of MA 956 and Cabot-214 with published data for HAYNES[4] alloy No. 188 (Haynes 188) (ref. 5) and Inconel 617 (refs. 5 and 8). Haynes 188 and Inconel 617 were high nickel-chromium-content alloys that formed mixed oxides of Ni and Cr and generally had high-temperature emittances of about 0.8, as shown in figure 10. The emittance for MA 956 and Cabot-214 was significantly less than 0.8, which is the accepted minimum value for TPS surfaces. The low emittance of MA 956 and Cabot-214 points to the need for emittance enhancement of the surface oxide layer in the wavelength region below 10 μm to assure their successful use in heat shield applications.

Concluding Remarks

The oxidation and emittance characteristics of INCOLOY alloy MA 956 (MA 956), an iron-base oxide-dispersion-strengthened alloy, and CABOT alloy No. 214 (Cabot-214), an alumina-forming nickel-chromium alloy, were evaluated for thermal protection system applications in advanced reentry vehicles. The oxidation resistance of MA 956 and Cabot-214 was good compared with that of other superalloys. Although MA 956 formed some hematite that was eventually lost and the α-Al_2O_3 layer in Cabot-214 formed a potentially deleterious solid solution with chromium from the substrate metal, neither alloy experienced any significant failure of the protective α-Al_2O_3 layer. The emittance values of these alloys (0.7 for MA 956 and 0.6 for Cabot-214) were significantly below the goal of 0.8 set for thermal protection system surfaces. This indicates the need to develop high-emittance coatings that will not degrade the excellent oxidation resistance of alloys of this type.

[4] HAYNES: Trademark of the Cabot Corporation.

NASA Langley Research Center
Hampton, VA 23665-5225
March 10, 1986

References

1. Varisco, Angelo; Bell, Paul; and Wolter, Willy: *Design and Fabrication of Metallic Thermal Protection Systems for Aerospace Vehicles.* NASA CR-145313, 1978.
2. Stewart, David A.; Rakich, John V.; and Lanfranco, Martin J.: Catalytic Surface Effects on Space Shuttle Thermal Protection System During Earth Entry of Flights STS-2 Through STS-5. *Shuttle Performance: Lessons Learned*, James P. Arrington and Jim J. Jones, compilers, NASA CP-2283, Part 2, 1983, pp. 827–845.
3. Blair, W.; Meaney, J. E.; and Rosenthal, H. A.: *Fabrication of Prepackaged Superalloy Honeycomb Thermal Protection System (TPS) Panels.* NASA CR-3755, 1985.
4. Cunnington, G. R.; Fretter, E. F.; and Clark, R. K.: Radiative Properties of a Nickel Based Superalloy—Inconel 617—After Simulated Earth Reentry. AIAA-82-0898, June 1982.
5. Cunnington, G. R.; Funai, A. I.; and McNab, T. K.: *Radiative Properties of Advanced Spacecraft Heat Shield Materials.* NASA CR-3740, 1983.
6. Lowell, Carl E.; and Deadmore, Daniel L.: *High Velocity Oxidation and Hot Corrosion Resistance of Some ODS Alloys.* NASA TM X-73656, [1977].
7. Clark, Ronald K.; and Cunnington, George R., Jr.: Vapor Deposited Emittance/Catalysis Coatings for Superalloys in Heatshield Applications. AIAA-85-0403, Jan. 1985.
8. Clark, Ronald K.; and Unnam, Jalaiah: Response of Inconel 617 to Sea Salt and Re-Entry Conditions. *J. Spacecr. & Rockets*, vol. 23, no. 1, Jan.-Feb. 1986, pp. 96–101.
9. Wiedemann, K. E.; and Unnam, J.: A Method of Rapidly Obtaining Concentration-Depth Profiles From X-Ray Diffraction. *J. Appl. Phys.*, vol. 58, no. 3, Aug. 1, 1985, pp. 1095–1101.
10. Gulbransen, Earl A.; and Jansson, Sven A.: Vaporization Chemistry in the Oxidation of Carbon, Silicon, Chromium, Molybdenum and Niobium. *Heterogeneous Kinetics at Elevated Temperatures*, G. R. Belton and W. L. Worrell, eds., Plenum Press, 1970, pp. 181–208.
11. Richards, R. G.; and White, J.: Phase Relationships of Iron-Oxide-Containing Spinels. *Part II. Relationships in the Systems Fe-Cr-O, Fe-Mg-O, Fe-Al-Cr-O, and Fe-Al-Cr-Mg-O.* Trans. British Ceram. Soc., vol. 53, no. 7, July 1954, 422–459.
12. Touloukian, Y. S.; and DeWitt, D. P., eds.: *Thermal Radiative Properties—Nonmetallic Solids.* IFI/Plenum, 1972.

TABLE I. NOMINAL CHEMICAL ANALYSES OF MA 956 AND CABOT-214

MA 956		Cabot-214	
Element	Weight, percent	Element	Weight, percent
Fe	75.5	Ni	76.5
Cr	19.3	Cr	16.0
Al	4.3	Al	4.5
[a]Y	.5	Fe	3.0
Ti	.4	[b]Y	.04

[a]Present as Y_2O_3 in MA 956.
[b]Maximum.

TABLE II. HYMETS OPERATING CONDITIONS FOR SIMULATED REENTRY EXPOSURE OF SPECIMENS

Specimen surface temperature, °C	1095
Surface pressure, Pa	800
Free-stream Mach number	3.5
Free-stream enthalpy, MJ/kg	9
Cold-wall heating rate, kW/m^2	300

TABLE III. PHASES IN THE INITIAL AND SIMULATED REENTRY EXPOSED MA 956 AND CABOT-214 AS IDENTIFIED BY X-RAY DIFFRACTION

Alloy	Initial product	After 0.5 hr	After 7.5 hr
MA 956	α-(Fe-Cr-Al-Ti)	α-(Fe-Cr-Al-Ti)	α-(Fe-Cr-Al-Ti)
	α-Al_2O_3 (corundum)	α-Al_2O_3	α-Al_2O_3
	[a] α-$(Fe,Al,Cr,Ti)_2O_3$	α-$(Fe,Al,Cr,Ti)_2O_3$	
Cabot-214	$(\gamma + \gamma')$-(Ni-Cr-Al-Fe)	$(\gamma + \gamma')$-(Ni-Cr-Al-Fe)	$(\gamma + \gamma')$-(Ni-Cr-Al-Fe)
	α-Al_2O_3	α-Al_2O_3	[b] α-$(Al_2O_3$-$Cr_2O_3)$
	[c] α-$(Al,Cr)_2O_3$		

[a]Solid solution of Fe_2O_3, Al_2O_3, Cr_2O_3, and Ti_2O_3. It is essentially α-Fe_2O_3 (hematite), but the exact composition is uncertain.

[b]Solid solution whose composition varied from 50 molar percent α-Cr_2O_3 at the metal-oxide interface to 100 percent α-Al_2O_3 at the free surface.

[c]Solid solution of 50 molar percent α-Cr_2O_3 and 50 molar percent α-Al_2O_3.

TABLE IV. EDXA COUNTS FOR MA 956 AND CABOT-214 IN VARIOUS CONDITIONS

(a) MA 956

Region	EDXA counts for—		
	Al	Fe	Cr
Initial:			
Small spheres	478×10^2	43×10^2	22×10^2
After 1 cycle:			
Small spheres	455×10^2	66×10^2	25×10^2
Large spheres	48	348	15
Between spheres	294	119	53
After 15 cycles:			
Small spheres	505×10^2	24×10^2	22×10^2
Between spheres	378	93	44

(b) Cabot-214

Region	EDXA counts for—			
	Al	Cr	Ni	Fe
Initial:				
Bright region	290×10^2	59×10^2	128×10^2	3×10^2
Dark region	82	103	260	10
After 1 cycle:				
Bright region	310×10^2	56×10^2	116×10^2	4×10^2
Dark region	330	35	105	3
After 15 cycles:				
Bright region	440×10^2	3×10^2	5×10^2	0
Dark region	370	28	57	0

TABLE V. SUMMARY OF NEAR-NORMAL EMITTANCE RESULTS FOR MA 956 AND CABOT-214 ALLOYS

[Blank spaces indicate that no data were taken]

Material	Specimen	[a]Reentry exposure time, hr	Initial emittance			Final emittance		
			Room temperature		1095°C	Room temperature		1095°C
			[b]DB100	[c]Summed	[c]Summed	[b]DB100	[c]Summed	[c]Summed
MA 956	M590	0	0.54	0.56	0.69	0.54	0.56	0.69
	M582	.5				.53	.58	.72
	M527	.5	.48			.52	.57	.71
	M562	2.5	.51			.56	.59	.72
	M504	5.0	.47			.52	.58	.66
	M513	7.5	.49			.55	.58	.71
	M506	7.5	.46			.53	.55	.67
	M514	7.5	.47			.55	.58	.74
Cabot-214	C15	0	0.41	0.43	0.65	0.41	0.42	0.65
	C30	0		.43	.64		.43	.64
	C18	.5	.45			.46	.48	.60
	C87	2.5	.50			.51	.54	.62
	C8	5.0	.48			.49	.53	.61
	C90	7.5				.48	.51	.58
	C52	7.5	.36			.43	.48	.54
	C76	7.5	.46			.49	.52	.60

[a]Exposure time was comprised of 0.5-hr tests under simulated reentry conditions at 1095°C.

[b]Gier-Dunkle DB100 room-temperature total-reflectance reflectometer.

[c]Total emittance was calculated using room-temperature spectral reflectance data from a Perkin-Elmer Model 330 spectrophotometer with Hitachi Model 320 integrating sphere and a Gier Dunkle Model HCDR 3 heated-cavity spectral-reflectance reflectometer.

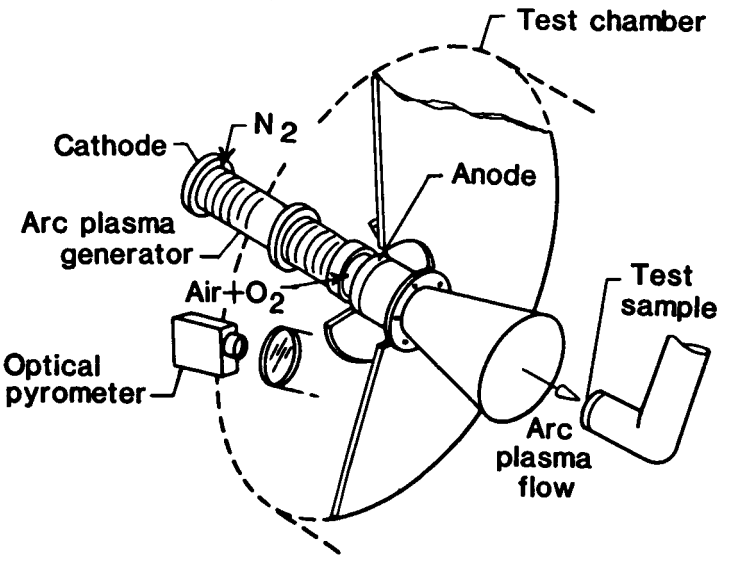

Figure 1. Schematic diagram of the HYMETS facility.

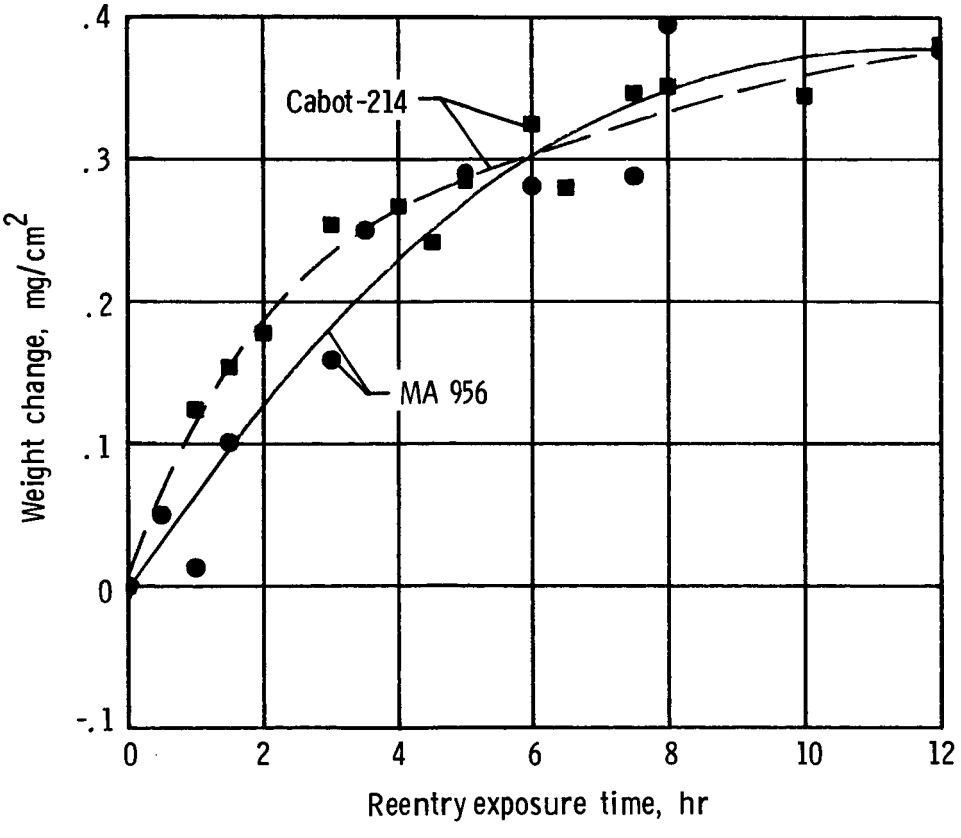

Figure 2. Weight change of MA 956 and Cabot-214 during exposure to simulated reentry conditions at 1095°C.

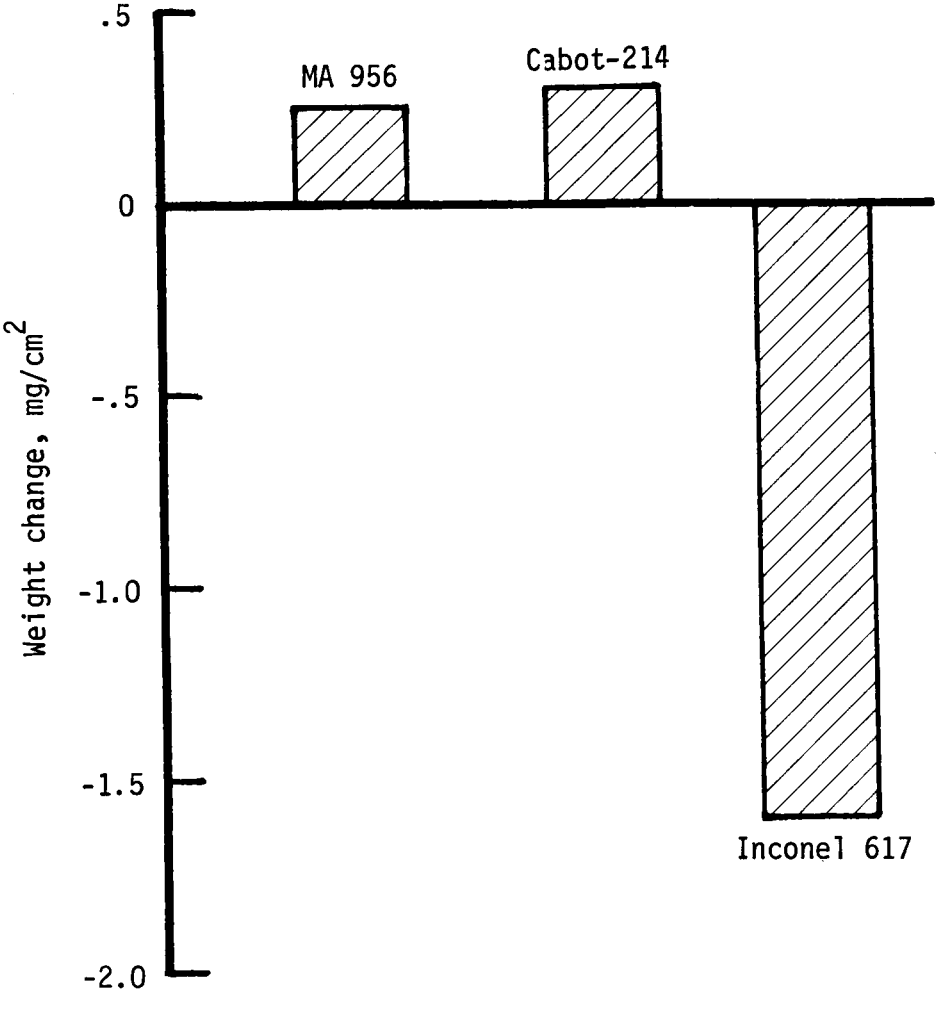

Figure 3. Comparison of weight change for different alloys after simulated reentry exposure of 5 hr at 1095°C.

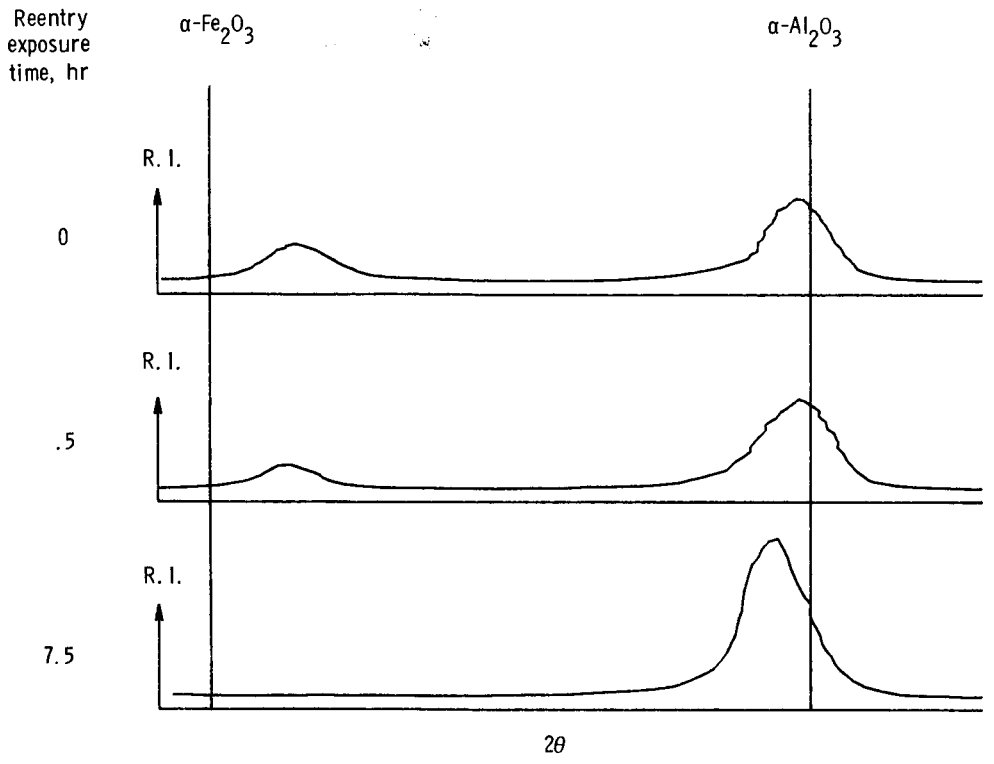

Figure 4. Composition changes in the surface oxide on MA 956 with reentry exposure time, as determined by X-ray diffraction analysis.

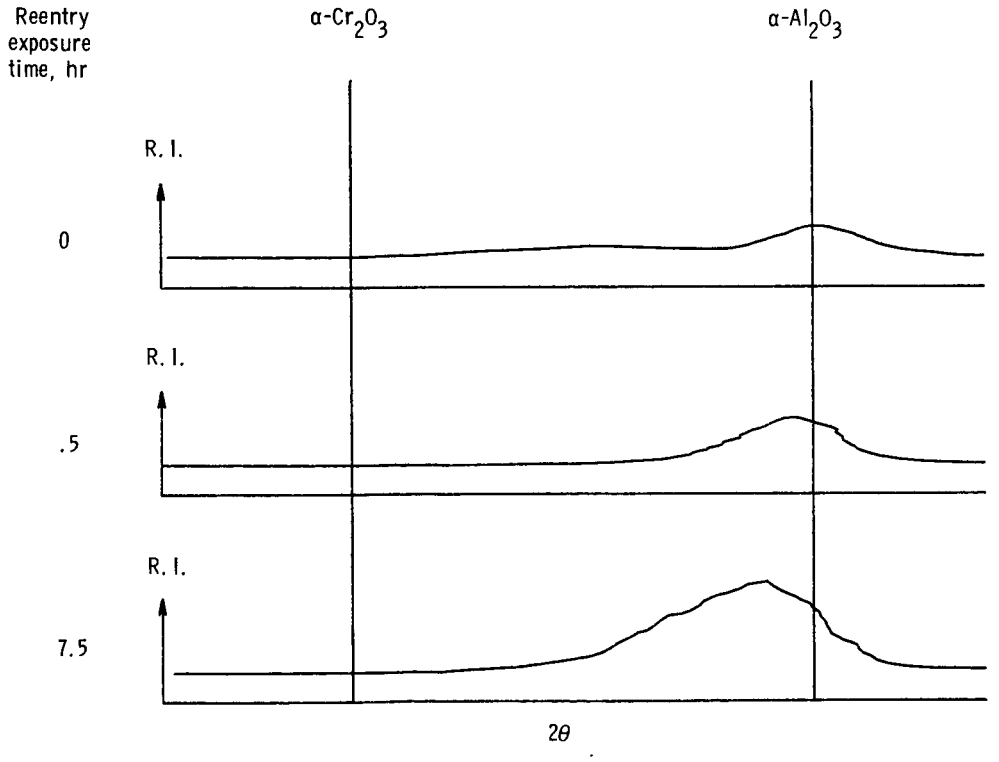

Figure 5. Composition changes in the surface oxide on Cabot-214 with exposure time, as determined by X-ray diffraction analysis.

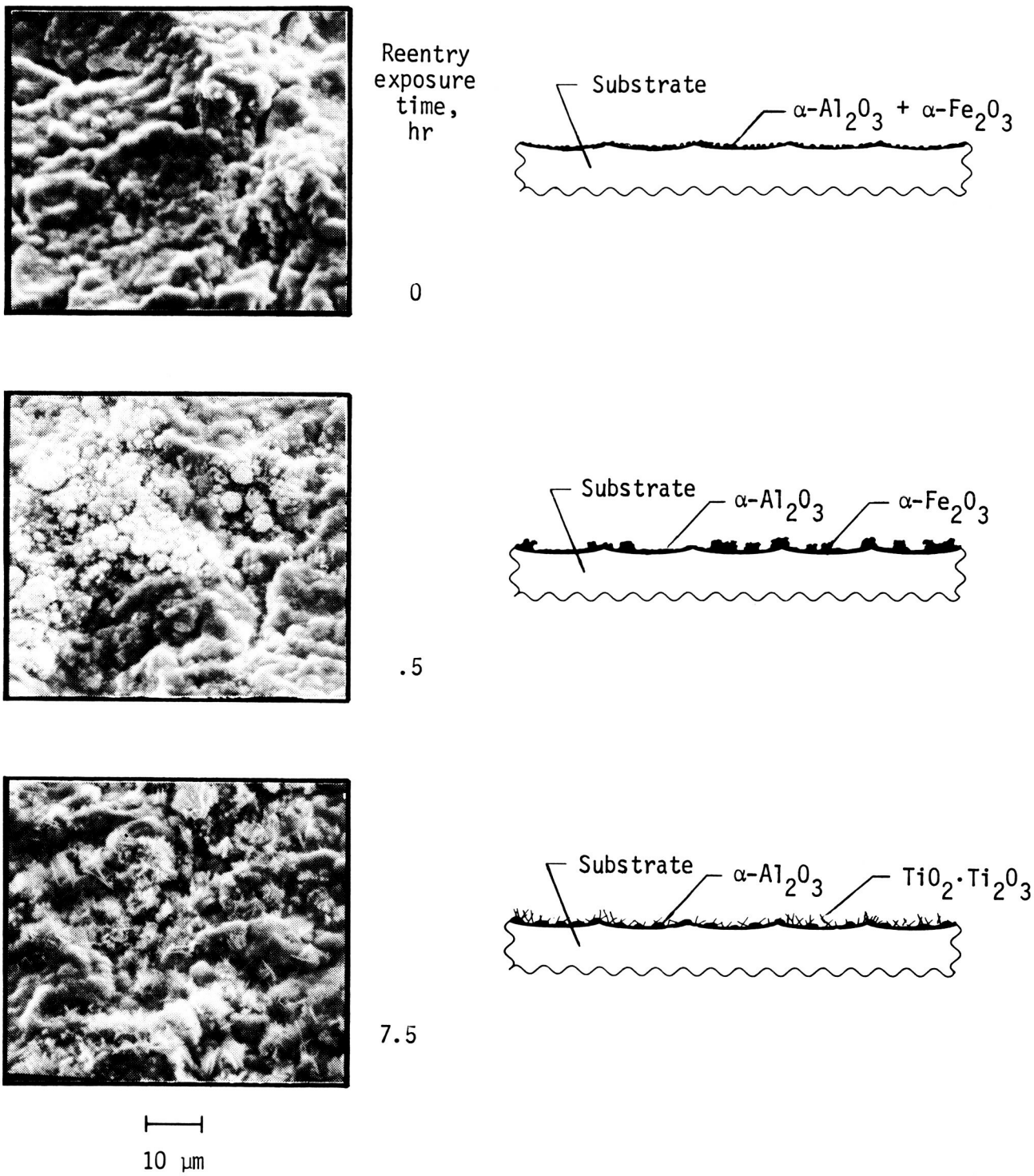

L-86-317

Figure 6. Changes in surface morphology of MA 956 after simulated reentry exposures.

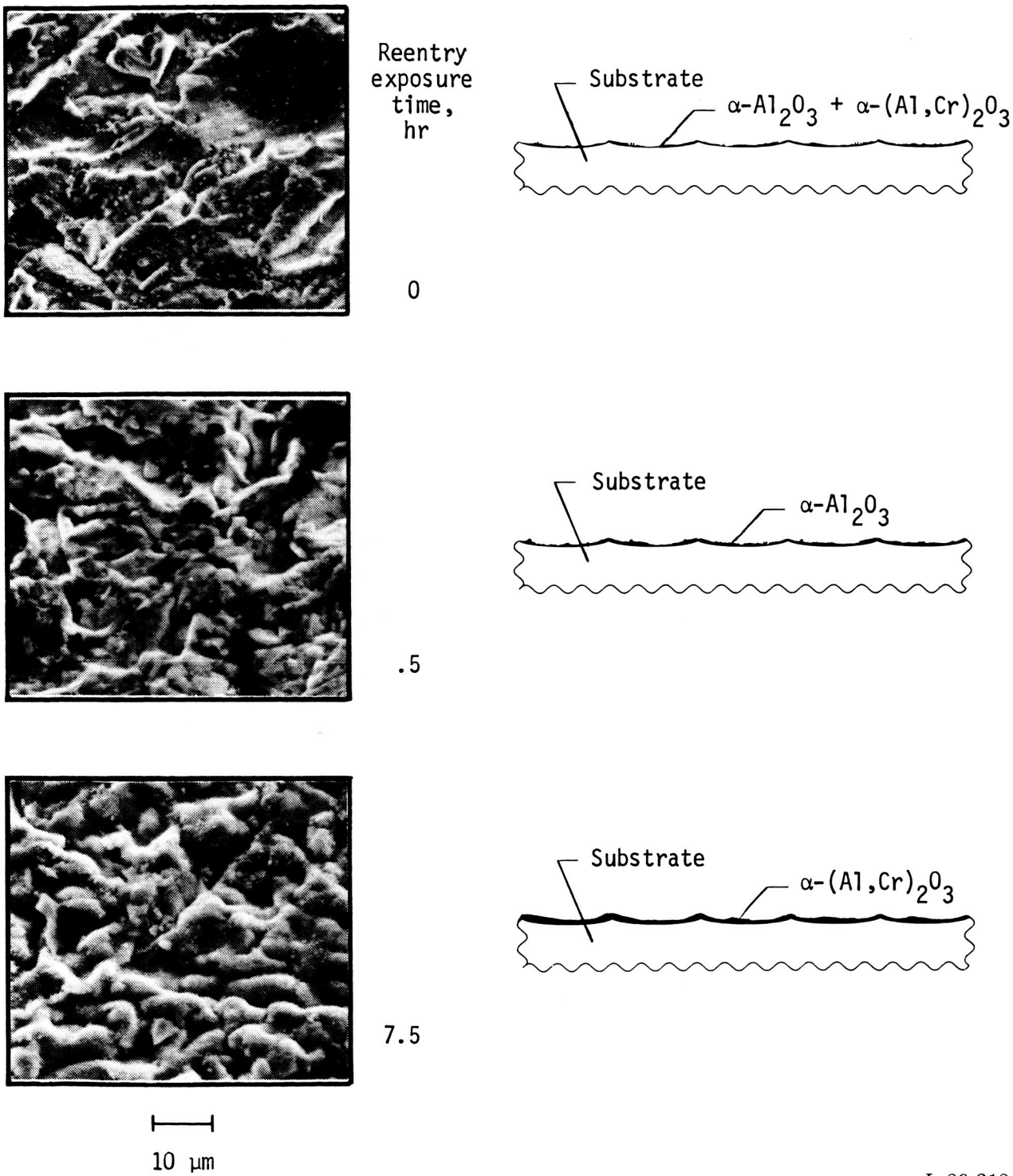

L-86-318

Figure 7. Changes in the surface morphology of Cabot-214 after simulated reentry exposures.

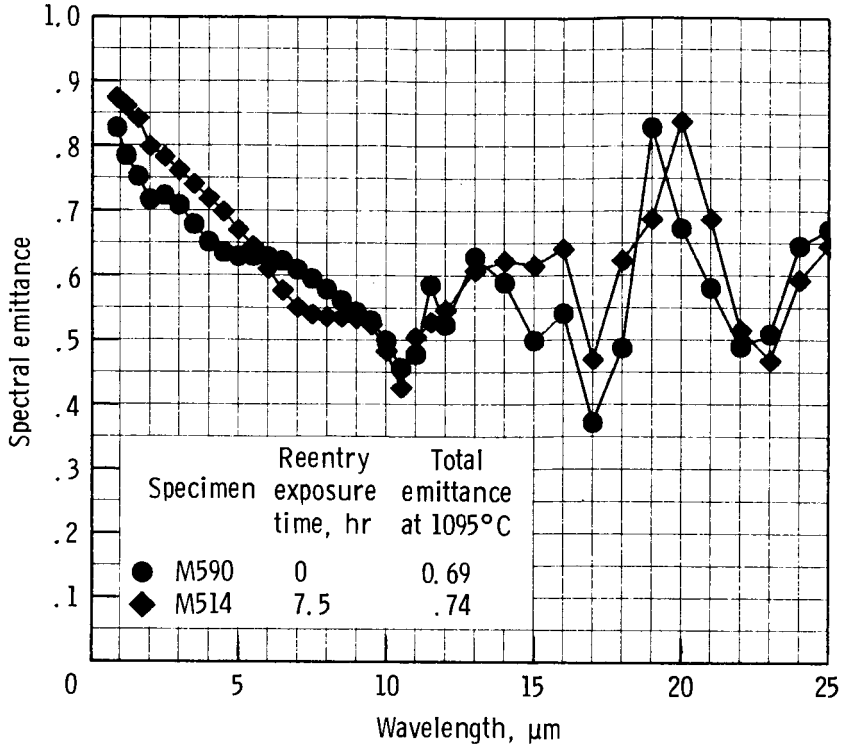

Figure 8. Variation in room-temperature spectral emittance of MA 956 with reentry exposure time.

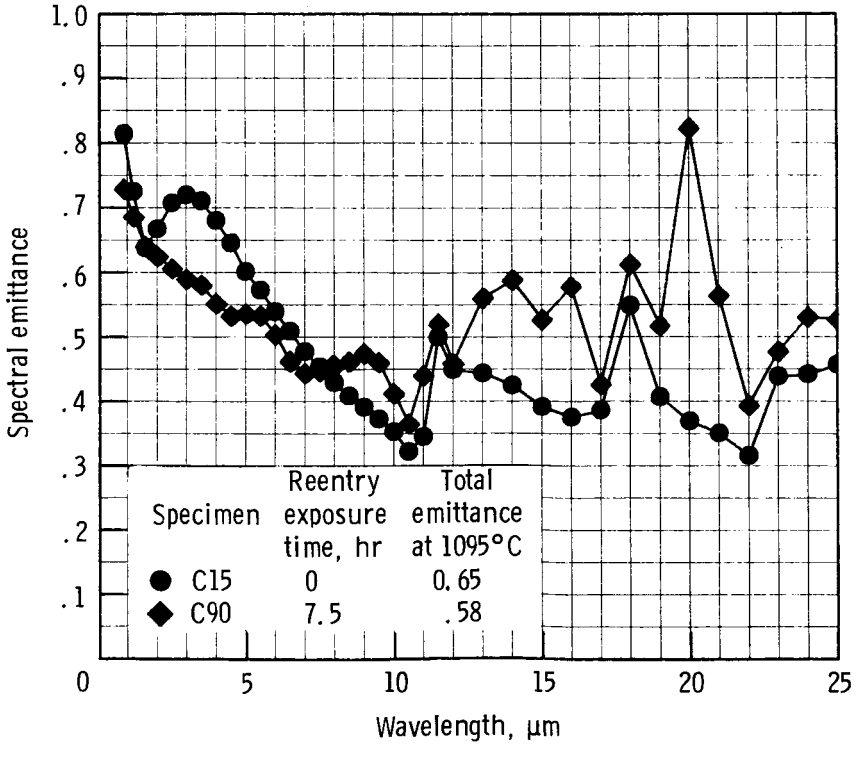

Figure 9. Variation in room-temperature spectral emittance of Cabot-214 with reentry exposure time.

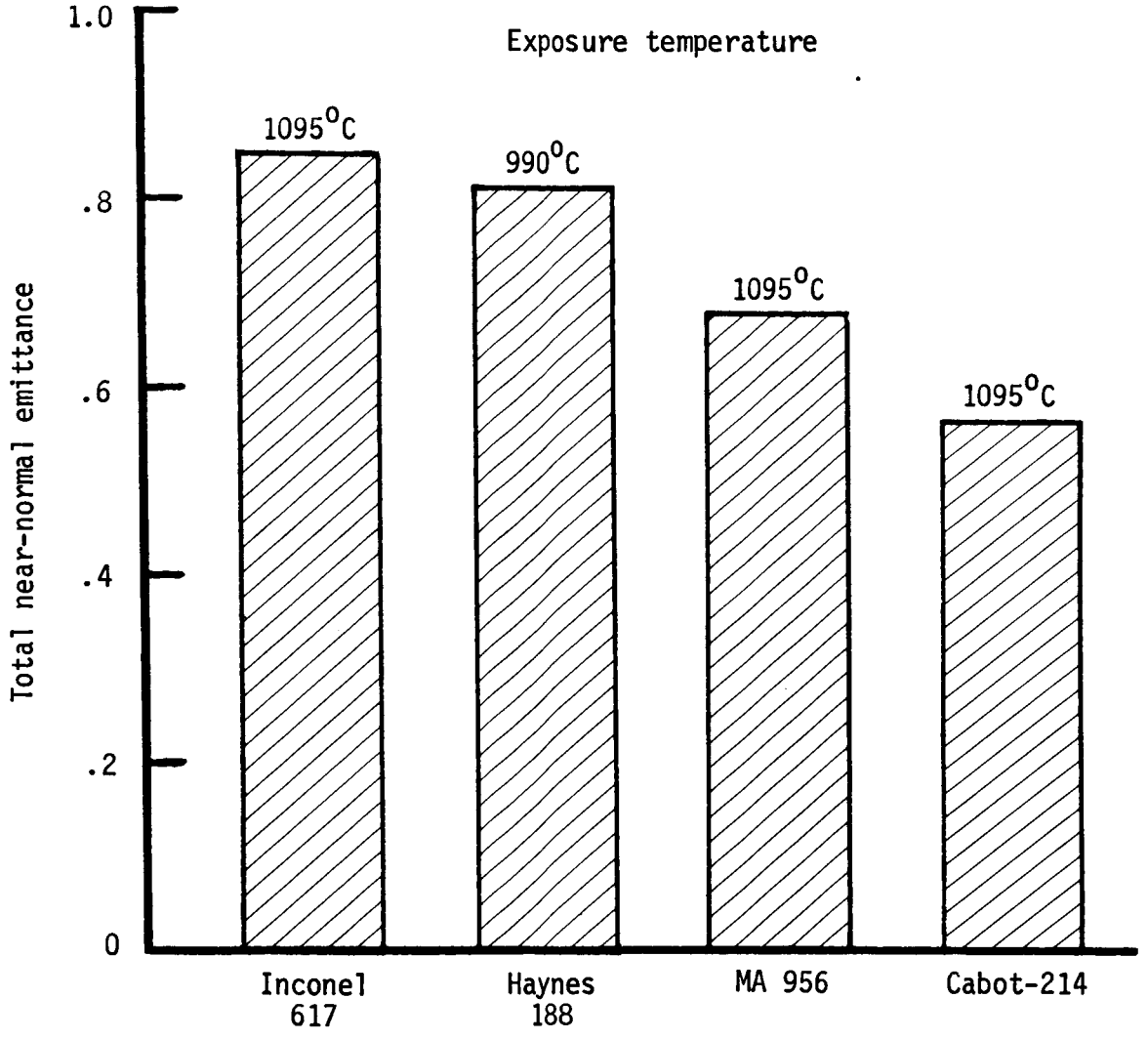

Figure 10. Comparison of emittance at exposure temperature for MA 956 and Cabot-214 with literature results for other alloys.

Standard Bibliographic Page

1. Report No.	2. Government Accession No.	3. Recipient's Catalog No.
NASA TP-2578		

4. Title and Subtitle	5. Report Date
Oxidation and Emittance of Superalloys in Heat Shield Applications	June 1986
	6. Performing Organization Code
	506-43-81-01
7. Author(s)	8. Performing Organization Report No.
Karl E. Wiedemann, Ronald K. Clark, and Jalaiah Unnam	L-16104
9. Performing Organization Name and Address	10. Work Unit No.
NASA Langley Research Center Hampton, VA 23665-5225	
	11. Contract or Grant No.
12. Sponsoring Agency Name and Address	13. Type of Report and Period Covered
National Aeronautics and Space Administration Washington, DC 20546-0001	Technical Paper
	14. Sponsoring Agency Code

15. Supplementary Notes

Karl E. Wiedemann and Jalaiah Unnam: Analytical Services and Materials, Inc., Hampton, Virginia.
Ronald K. Clark: Langley Research Center, Hampton, Virginia.
Results were presented at the 1985 TMS-AIME Fall Meeting, October 13–17, 1985, Toronto, Canada.

16. Abstract

Recently developed superalloys that form alumina coatings have a high potential for heat shield applications for advanced aerospace vehicles at temperatures above 1095°C. Both INCOLOY alloy MA 956 (of the Inco Alloys International, Inc.), an iron-base oxide-dispersion-strengthened alloy, and CABOT alloy No. 214 (of the Cabot Corporation), an alumina-forming nickel-chromium alloy, have good oxidation resistance and good elevated temperature strength. The oxidation resistance of both alloys has been attributed to the formation of a thin alumina layer (α-Al_2O_3) at the surface. Emittance and oxidation data were obtained for simulated Space Shuttle reentry conditions using a hypersonic arc-heated wind tunnel. The surface oxides and substrate alloys were characterized using X-ray diffraction and scanning and transmission electron microscopy with an energy-dispersive X-ray analysis unit. The mass loss and emittance characteristics of the two alloys are discussed.

17. Key Words (Suggested by Authors(s))	18. Distribution Statement
Superalloys Oxidation Heat shields Reentry Oxide-dispersion-strengthened alloys Emittance	Unclassified—Unlimited Subject Category 26

19. Security Classif.(of this report)	20. Security Classif.(of this page)	21. No. of Pages	22. Price
Unclassified	Unclassified	19	A02

For sale by the National Technical Information Service, Springfield, Virginia 22161

NASA-Langley, 1986